Type of contribution:
Editorial
▶ Research Paper
Case Study
Review Paper
Scientific Data
Report of Tech. Application

mesi
e-issn. 2798-5245

Mechanical Engineering for Society and Industry
Vol. 4, No. 2 (2024) pp 223-236
https://doi.org/10.31603/mesi.11945

Optimization of preparation parameters of palm oil-based nanofuel with MWCNT for stability using Taguchi-grey relation analysis (GRA) combination

Imam Muda Nauri, Andoko*, Riduwan Prasetya, Muhammad Faizullah Pasha, Muhamad Rizky Akbar, Muhammad Wahid Darmawan, Poppy Puspitasari

Department of Mechanical and Industrial Engineering, State University of Malang, Malang 65145, **Indonesia**
✉ andoko.ft@um.ac.id

This article contributes to:
7 AFFORDABLE AND CLEAN ENERGY
SUSTAINABLE DEVELOPMENT GOALS

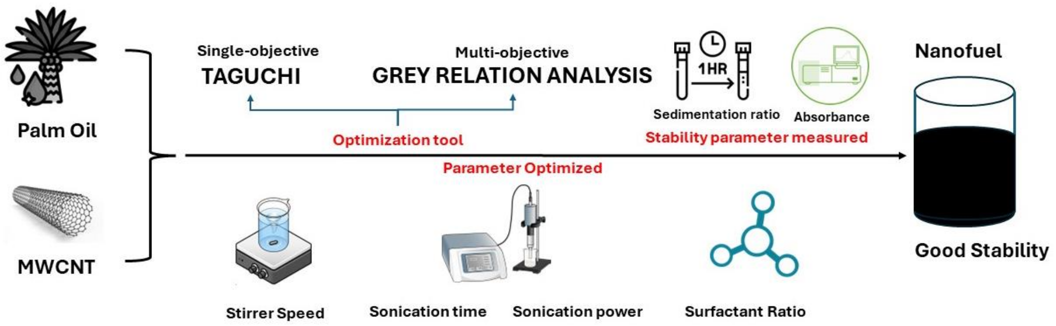

Highlights:

- Employed Taguchi method for single-objective optimization and Grey Relational Analysis (GRA) for multi-objective optimization to enhance nanofuel stability.
- Identified that surfactant concentration has the highest impact on nanofuel stability, contribute up to 82.60%.
- Consistency in optimal parameters across both Taguchi and GRA methods validates the reliability of the optimization process.
- Provides a strong foundation for developing more stable nanofuels, potentially enhancing energy efficiency and sustainability, with practical guidelines for real-world applications.

Article info
Submitted: 2024-07-28
Revised: 2024-12-01
Accepted: 2024-12-11

Publisher
Universitas Muhammadiyah Magelang

Abstract

This research optimizes the preparation parameters of palm oil-based nanofuel and Multi Wall Carbon Nanotube (MWCNT) to produce stable nanofuel. The parameters optimized include stirrer speed, sonication time, sonication power, and surfactant ratio, with stability measured through absorbance and sedimentation ratio (SR). The Taguchi method, using an L9 orthogonal array designed with minitab 19.0 software, was employed for single-objective optimization, while Grey Relation Analysis (GRA) is applied for multi-objective optimization. Experimental results show that the optimal conditions for absorbance are stirrer speed of 1000 rpm, sonication time of 30 minutes, sonication power of 200 watts, and surfactant ratio of 1, whereas for sedimentation ratio the optimal conditions are stirrer speed of 1000 rpm, sonication time of 30 minutes, sonication power of 150 watts, and surfactant ratio of 1. ANOVA analysis reveals that surfactant concentration contributes the most to nanofuel stability, with contributions of 79.63% for absorbance and 82.60% for sedimentation ratio. Multi-objective GRA optimization results also show that surfactant concentration is the most dominant factor, contributing 71.5% to the Grey Relational Grade (GRG). The consistency of optimal parameters yielded by both Taguchi and GRA methods reinforces the validity and consistency of this study's results. This research provides a strong foundation for the development of more stable nanofuels, potentially enhancing energy efficiency and sustainability. These findings offer practical guidelines for real-world applications and make significant contributions to nanofuel technology.

Keywords: Nanofuel; Optimization; Taguchi; GRA; MWCNT; Palm oil

1. Introduction

Decreasing fossil fuel reserves and increasing environmental concerns necessitate a shift to more sustainable and environmentally friendly energy sources [1]–[4]. The fossil fuels that have driven industrial growth are not only depleting rapidly but also contributing significantly to environmental pollution and global warming [5]–[7]. Because of their sustainable nature and smaller environmental impact, renewable energy sources such as biodiesel provide a promising alternative [8]–[12]. Biodiesel is an alternative energy source that may be made from a range of easily obtained basic materials, including different vegetable oils, animal fats, and recycled cooking oil [13], [14].

Palm oil holds significant potential as a biodiesel fuel due to its renewable and beneficial properties. Biodiesel derived from palm oil, particularly Crude Palm Oil (CPO), has been proven to meet various fuel standards and shows promising characteristics for diesel engines. Research has demonstrated that palm oil biodiesel can be produced through transesterification, yielding high-purity methyl esters, especially when co-solvents such as Tetrahydrofuran (THF) are used, achieving purity levels of up to 94.09% [15]. The performance of palm oil biodiesel in internal combustion engines has been extensively analyzed, showing that biodiesel can be blended with diesel in various proportions without requiring engine modifications. These blends enhance mechanical efficiency and reduce Carbon Monoxide (CO), Hydrocarbons (HC), and Nitrogen Oxide (NOx) emissions compared to pure diesel, making them environmentally friendly and sustainable [16]. For instance, palm oil biodiesel blends like B10 have demonstrated impressive brake thermal efficiency and can be used as a substitute fuel in four-cylinder agricultural tractor engines without modifications [17]. Biodiesel derived from palm oil, particularly CPO, has been proven to meet various fuel standards and shows promising characteristics for diesel engines. Biodiesel blends are commonly categorized based on their composition, where B5 represents a mixture of 5% biodiesel with 95% petroleum diesel, while B10 contains 10% biodiesel and 90% petroleum diesel. These blends have shown that their density and viscosity values fall within acceptable ranges, ensuring good engine performance [18]. However, when directly applied to diesel engines, pure palm oil biodiesel presents certain drawbacks. These include lubricating oil degradation, higher friction coefficients, more severe downforce, and lower brake torque, leading to significant mechanical and performance weaknesses in diesel engines. This is due to high density, low fuel atomization, low flash and boiling points, and cold ignition issues associated with palm oil biodiesel, which require modifications for optimal use [18]. Despite these challenges, the overall benefits of palm oil biodiesel, such as emission reduction and increased engine efficiency, make it a viable alternative to fossil fuels, contributing to environmental sustainability and energy security.

An alternative solution to the biodiesel problem, of which is to combine it with nanoparticles [19]–[21]. Titanium dioxide (TiO_2) mixed in biodiesel has shown improvements in performance and emission characteristics with lower Specific Fuel Consumption (SFC) when blended at different concentrations [22]. Similarly, Pithecellobium dulce seed oil biodiesel mixed with titanium oxide and aluminium oxide nanoparticles has shown effective catalytic potential in biodiesel combustion [23]. Additionally, Cerium xide (CeO_2) nanoparticles blended with Waste Cooking Oil (WCO) biodiesel resulted in increased Brake Thermal Efficiency (BET) and reduced NOx, CO, and CO_2 emissions with optimal performance at a concentration level of 50 ppm [24]. Graphene nanoparticles have also been investigated, particularly in ternary blends with ethanol and biodiesel, showing significant improvements in engine performance and reductions in CO, unburned hydrocarbons, NOx, and smoke levels [25]. Specifically for palm oil-derived biodiesel, the incorporation of Multi Wall Carbon Nanotubes (MWCNT) has shown significant improvements in various properties. MWCNTs mixed with palm oil behave as Newtonian fluids regardless of concentration and temperature, with a significant increase in viscosity index by 16% at a concentration of 1% wt [26]. Research by Nurmukan et al. [27], found that the addition of MWCNTs can enhance combustion characteristics, such as increasing laminar burning velocity and blow-off velocity, and extending flammability limits under both lean and rich fuel conditions. Additionally, Amsal et al. [28] demonstrated that the evaporation characteristics of palm oil biodiesel can be improved with MWCNTs, particularly those with smaller diameters, which significantly increase the evaporation constant at various temperatures and show better heat transfer properties. Seela et al. [29], indicate that biodiesel and MWCNT blends show improved brake-specific fuel consumption and brake thermal efficiency, along with reductions in emissions such as NOx and CO_2. Overall, integrating MWCNTs into palm oil biodiesel enhances thermal and combustion properties while also contributing to more efficient fuel usage.

Many studies have shown that nanoparticles combined with biodiesel offer remarkable advantages in combustion applications. Nanofuels not only improve thermal and mass transport properties but also facilitate more uniform and controlled combustion. Nevertheless, issues with nanofuels, such as agglomeration, clogging, and nanoparticle sedimentation in fluids, can affect stability and combustion performance. Stability of nanofuels is a crucial factor in practical applications, especially in internal combustion engines, because instability can lead to nanoparticle agglomeration and sedimentation, which can damage engine components and reduce fuel efficiency. Various studies have explored different methods to enhance nanofuel stability. Shaikh et al. [30] investigated the solubility and stability of diesel-ethanol-nanoparticle blends and found that a combination of low ultrasonication time (15 minutes) and high stirring speed (2500-4000 rpm) without surfactant significantly improved ethanol solubility in diesel, while ZnO nanoparticles showed higher stability compared to Al_2O_3 nanoparticles under the same conditions. Rao et al. [31] highlighted the potential of magnetite nanoparticles due to their high surface area, thermal conductivity, and ease of exhaust gas separation, which also contributed to improved fuel stability and reduced emissions. Saleem et al. [32] used UV-Vis spectral absorbance to measure the stability of cerium oxide nanofluids, noting that high-speed mixing followed by 40 minutes of ultrasonication produced a stable nanofuel solution for up to eight days. Bao et al. [33] examined the macroscopic spray characteristics of diesel-ethanol blends with cerium oxide nanoparticles, finding that the addition of nanoparticles increased spray penetration and cone angle, indicating improved fuel stability and combustion performance. Singh et al. [34] employed non-invasive and low-cost methods to analyze the sedimentation rate of various nanofuels, finding that metal oxides such as copper oxide and aluminum oxide exhibited a metastable state during sedimentation, underscoring the importance of initial concentration and column height in maintaining stability. Collectively, these studies underscore the importance of optimizing mixing parameters, types of nanoparticles, and concentrations to achieve stable nanofuels suitable for diesel engine applications.

Based on previous research on nanoparticles added to fuels, the stability of nanoparticles in nanofuels, particularly in palm oil biodiesel and MWCNTs, has not been well evaluated. The stability of the modified fuel blend must be ensured and evaluated to be recommended as an alternative fuel for diesel engines. Therefore, this study aims to evaluate the preparation process of nanofuel with respect to the resulting stability. The parameters optimized are the preparation parameters of nanofuel, including stirrer speed, sonication time, sonication power, and surfactant ratio. These parameters were chosen due to the ease of the preparation process. Evaluation is conducted using an optimization approach with the Taguchi method, which has been widely used to evaluate nanofluids. Stability is a crucial parameter to produce uniform nanofuel properties. For this purpose, multi-objective optimization using Grey Relational Analysis (GRA) is employed to prepare nanofuel, resulting in the best combination of preparation parameters. The results of this study are expected to contribute to the preparation of palm oil and MWCNT mixtures as nanofuel.

2. Material and Methods

2.1. Preparation of Nanofuel

Table 1. Properties of palm oil

Parameter	Value
Density at 25 °C [kg/m^3]	872
Kinematic Viscosity at 40 °C [mm^2/s]	4.1
Flash Point [°C]	101
Boiling Point [°C]	>210
Cetane number	51
Weight moleculer [g/mol]	281
High heating value [MJ/kg]	39.9

Table 2. Properties of MWCNT

Parameter	Value
Purity	98
Outer diameter (nm)	20-40
Inner diameter (nm)	5-12
Length (μm)	10-20
Specific surface area (m^2/g)	>60
Density ($g/(cm^3)$)	2.1
Number of walls	27-67

Nanofuel is made from palm oil and Multi Wall Carbon Nanotube (MWCNT). The palm oil was obtained from PT Batara Elok Semesta Terpadu (Gresik, Indonesia), with its thermophysical properties shown in **Table 1**. The MWCNT nanoparticles were purchased from XFNANO (China), with properties listed in **Table 2**. SPAN80 as the surfactant was obtained from Sigma Aldrich.

Nanofuel is prepared by adding MWCNT to palm oil. MWCNT at a concentration of 200 ppm and SPAN 80 at varying concentrations (0-1) are weighed using a precision scale and added to 300 mL of palm oil. The mixture is stirred with a magnetic stirrer at room temperature for 15 minutes at different stirring speeds (1000-1500 rpm). Subsequently, the mixture is sonicated using an ultrasonic homogenizer (Labocon, LUH-103) at different power levels (100-200 W), sonication times (30-60 minutes), a constant frequency (20 kHz), and an on-off sonication period of 3 seconds on and 8 seconds off.

2.2. Measurement of Nanofuel Stability

Sedimentation of nanoparticles in nanosuspension is a natural phenomenon caused by gravity, leading to aggregation among particles. Sedimentation is a simple method to evaluate the stability of nanofluids. The sedimentation height can be recorded over time using visual techniques. The sedimentation ratio (SR) can be obtained by comparing the sedimentation height (H_S) to the total sample height (H_T) [35].

$$SR = \frac{H_S}{H_T} \tag{1}$$

The deposition of particles that show flocculation-type sedimentation is caused by the consolidation process. In this process, the fluid moves upward through various pores of the solid particle clusters. These clusters form distinct sediment layers and settle over time. The sediment layers further consolidate under their own weight as the upper sediment layers exert pressure on the lower layers.

The second method used to assess nanofuel stability is ultraviolet absorption using an Ultraviolet-Visible Spectrophotometer (UV-Vis). The UV-Vis spectrophotometer was first used by [36] to estimate the stability of carbon nanotube (CNT) suspensions. The distribution of nanoparticles in the suspension is characterized through the absorption spectrum because the optical properties of the particles depend on their morphology. There is a linear relationship between the absorption intensity and the nanoparticle concentration in the nanofluid [37]. The UV-Vis method shows good reliability for measuring nanosuspension stability [38]. The UV-Vis spectrophotometer used in this study is the Nanospectrophotometer UV-Vis with cuvette Implen NP80. While this study focuses on stability, future work should investigate potential trade-offs, such as the impact on fuel viscosity or combustion properties, to ensure comprehensive optimization.

2.3. Taguchi Experiment Design

The Taguchi method and ANOVA in this study were conducted using Minitab 19.0 software. The Taguchi method is used to determine the experimental design by considering the combination of factors to achieve optimal experiments while minimizing time, effort, and cost. Utilizing the loss function, the Taguchi method calculates the deviation between experimental values and target values. The Taguchi method was chosen because of its efficiency in minimizing the number of experiments required [39]–[44]. This approach uses orthogonal arrays to provide distinct guidelines from the analysis phase regarding influential parameters and appropriate levels. In this study, the combination of all nanofuel preparation processes with 4 parameter factors and 3 levels results in 81 experiments (3^4). The preparation process consisting of 4 factors and 3 levels uses the L_9 orthogonal array as shown in **Table 3**. The L9 orthogonal array was selected for its efficiency in reducing the number of experimental trials while maintaining sufficient statistical power. The sample size was determined based on preliminary tests to ensure the detection of significant differences in both sedimentation and absorption ratios. The selection of the orthogonal array is displayed in **Table 4**.

Table 3. Factor and experiment level

Factor	Code	Level		
		1	2	3
Stirrer speed (rpm)	A	1000	1250	1500
Sonication time (min)	B	30	45	60
Sonication power (watts)	C	100	150	200
Surfactant: MWCNT	D	0	0.5	1

Table 4. L9 Taguchi experimental design

Exp. No.	Factor			
	A	B	C	D
1	1	1	1	1
2	1	2	2	2
3	1	3	3	3
4	2	1	2	3
5	2	2	3	1
6	2	3	1	2
7	3	1	3	2
8	3	2	1	3
9	3	3	2	1

2.4. Single-objective Optimization

2.4.1. Signal to Noise Ratio

In the Taguchi method, experimental data are transformed into signal-to-noise (SN) ratios. The goal of the Taguchi approach is to minimize the impact of uncontrollable parameters (noise) while maximizing the influence of controllable parameters (signal). Within the SN ratio framework, there are various criteria such as "smaller is better," "nominal is better," and "larger is better." In line with the objectives of this study, the main goal is to achieve optimal nanofluid stability, characterized by the lowest sedimentation ratio (where smaller is better) and the highest absorption level (where larger is better). The 'smaller is better' criterion for sedimentation ratio and 'larger is better' criterion for absorption ratio were chosen as they directly reflect nanofuel stability. A smaller sedimentation ratio indicates reduced nanoparticle agglomeration, while a larger absorption ratio signifies better nanoparticle dispersion. Signal-to-noise (S/N) ratio simplifies multi-level optimization by reducing variability caused by uncontrollable factors. This approach ensures robust parameter selection, aligning with the study's stability goals. The S/N ratios for 'smaller is better' and 'larger is better' were calculated using standard equations [45]. To minimize bias, consistent methods were employed across all calculations, and results were cross-validated for accuracy.

Smaller is better:

$$n_{ij} = -10 \times \log\left(\frac{1}{n}\sum_{i=1}^{n} Y_i^2\right) \tag{2}$$

Larger is better:

$$n_{ij} = -10 \times \log\left(\frac{1}{n}\sum_{i=1}^{n} \frac{1}{Y_i^2}\right) \tag{3}$$

where Y is the result of an experiment, i and j is number of experiment.

2.4.2. Analysis of Variance (ANOVA)

ANOVA is a statistical technique for determining the contribution of each factor by analyzing the results obtained from orthogonal array experiments. In this study, ANOVA was conducted to explain the relative effects of different parameters in the nanofluid preparation process on stability, specifically regarding sedimentation and absorption ratio. ANOVA reliability was assessed using the F test (Fisher test) which was calculated using the equation [46].

$$SS_m = \frac{(\sum \eta_i)^2}{j} \tag{4}$$

$$SS_T = \sum \eta_i^2 - S_m \tag{5}$$

$$SS_A = \frac{(\sum \eta_{Ai}^2)^2}{N} - SS_m \tag{6}$$

$$SS_E = SS_T - \sum SS_A \tag{7}$$

$$V_A = \frac{SS_A}{f_A} \tag{8}$$

$$F_{A0} = \frac{V_A}{V_E} \tag{9}$$

where SS sum of squares, V variance, F F-test value, N number of repetitions, η SN ratio of performance characteristic, f degree of freedom, i level of factor, j number experiments in the orthogonal array, m the change, A the factor A, E the error, dan $A0$ test value of the factor. The significance threshold for p-values was set at 0.05, indicating a 95% confidence level. The F-test evaluates the relative contribution of each factor by comparing its variance to the error variance, ensuring the validity of the experimental results.

2.5. Multi-objective Optimization (Grey Relation Analysis)

Although the Taguchi technique is straightforward and efficient for parameter optimization, one of its limitations is that it can only be used for single-objective optimization. To overcome this limitation and facilitate the resolution of multi-objective optimization problems, one approach is to use Grey Relational Analysis (GRA) integrated with the Taguchi experimental design [45]. This method transforms multi-objective problems into a single-objective platform, allowing for the identification of optimal values from the converted single performance value. The steps for performing GRA are normalizing the experimental data, calculating the Grey Relation Coefficient (GRC), and calculating the Grey Relation Grade (GRG).

Normalization criteria, where "smaller is better," are given by Eq. (10) for the sedimentation ratio parameter, and "larger is better" are given by Eq. (11) for the absorption parameter [45].

$$x_i^*(k) = \frac{\max x_i^0(k) - x_i^0(k)}{\max x_i^0(k) - \min x_i^0(k)} \tag{10}$$

$$x_i^*(k) = \frac{x_i^0(k) - \min x_i^0(k)}{\max x_i^0(k) - \min x_i^0(k)} \tag{11}$$

where $x_i^*(k)$ is the measured results, $\max x_i^0(k)$ is the maximum value of $x_i^0(k)$, and $\min x_i^0(k)$ minimum value of $x_i^0(k)$, i is the number of experiment, and k is the quality characteristics. Then GRC is calculated using the equation (11). Δ_{0i} as following Eq. (12) is absolut value of the difference of the reference sequence ($x_0^*(k)$ and comparable sequence ($x_i^*(k)$). ζ is distinguish coefficients ranging between 0 to 1, and usually used 0.5. Δ_{min} and Δ_{max} is minimum and maximum value of Δ_{0i}.

$$\xi_i(k) = \frac{\Delta_{min} + \zeta\Delta_{max}}{\Delta_{0i}(k) + \zeta\Delta_{max}} \tag{12}$$

$$\Delta_{oi} = \left\| x_0^*(k) - x_i^*(k) \right\| \tag{13}$$

Finally, GRG is calculated by averaging the number of GRCs.

$$\gamma_i = \frac{1}{n}\sum_{k=1}^{n} \xi_i(k) \tag{14}$$

where γ_i changes in range 0 to 1 (usually 0.5), and n is the performance measure number.

3. Results and Discussion

3.1. Results of Taguchi Experiment

Absorbance (Abs) and Sedimentation Ratio (SR) were measured through the experimental design for each combination using the Taguchi method. Optimization was evaluated by controlling factors related to the signal-to-noise (SN) ratio. High absorbance and low sedimentation ratio are associated with good nanofuel stability; therefore, the "larger is better" equation is applied for absorbance, and the "smaller is better" equation is used for the sedimentation ratio. The SN ratio results for each process parameter are shown in **Table 5**.

3.2. Single-objective Optimization

3.2.1. Signal to Noise Ratio

The influence analysis of each control parameter (stirrer speed-A, sonication time-B, sonication power-C, surfactant ratio-D) on absorbance and sedimentation ratio is presented in the response table for SN. This table is created using the Taguchi technique, displaying the optimum parameters at each level of the independent variables for optimal dependent variables. The SN response table for absorbance is shown in **Table 6** and plotted in **Figure 1**. The best level for each control parameter is determined based on the highest SN value. Based on this, the best parameter levels are: parameter A (stirrer speed) at level 1 (1000 rpm, SN=3.9978), parameter B (sonication time) at level 1 (30 minutes, SN=2.9074), parameter C (sonication power) at level 3 (200 watts, SN=3.1962), and parameter D (surfactant ratio) at level 3 (1, SN=5.8446). For the sedimentation ratio, the SN response table is shown in **Table 7** and **Figure 2**. The best level for each control parameter is determined by the smallest SN value. Based on the results, the best parameter levels are: parameter A (stirrer speed) at level 1 (1000 rpm, SN=29.04), parameter B (sonication time) at level 1 (30 minutes, SN=28.57), parameter C (sonication power) at level 2 (150 watts, SN=28.58), and parameter D (surfactant ratio) at level 3 (1, SN=29.22).

The analysis results indicate that to achieve optimal nanofuel stability, both in terms of absorbance and sedimentation ratio (SR), specific combinations of surfactant ratio and sonication power must be considered. **Figure 3a** shows the contour plot for absorbance, where the highest values (S/N Abs > 6) are achieved with a surfactant ratio between 0.6 and 0.8 and sonication power ranging from 140 to 160 W. This indicates that these parameter combinations contribute significantly to the dispersion and stability of MWCNTs in palm oil. Meanwhile, **Figure 3b** presents the contour plot for the sedimentation ratio (SR). The lowest SR values (S/N SR > 35) are observed with a surfactant ratio of 0.6 to 0.8 and sonication power between 120 and 160 W, demonstrating that higher surfactant concentrations prevent sedimentation effectively. The consistency in the optimal parameter range between **Figure 3a** and **Figure 3b** highlights the robustness of the optimization process, as both metrics (absorbance and SR) indicate similar parameter dependencies.

Table 5. Experiment result

Exp. No.	Factor				Measurement		SN ratio	
	A	B	C	D	Abs	SR	Abs	SR
1	1	1	1	1	1.84	0.0556	5.29636	25.0985
2	1	2	2	2	0.92	0.0369	-0.72424	28.6595
3	1	3	3	3	2.35	0.0124	7.42136	38.1316
4	2	1	2	3	2.15	0.0141	6.64877	37.0156
5	2	2	3	1	1.86	0.0408	5.39026	27.7868
6	2	3	1	2	0.79	0.0344	-2.04746	29.2688
7	3	1	3	2	0.69	0.0230	-3.22302	32.7654
8	3	2	1	3	1.49	0.0228	3.46373	32.8413
9	3	3	2	1	1.36	0.0441	2.67078	27.1112

Table 6. Response table for SN ratio for Absorbance: (Larger is better *optimum level)

Level	A	B	C	D
1	**3.9978***	**2.9074***	2.2375	4.4525
2	3.3305	2.7099	2.8651	-1.9982
3	0.9705	2.6816	**3.1962***	**5.8446***
Delta	3.0273	0.2258	0.9587	7.8429
Rank	2	4	3	1

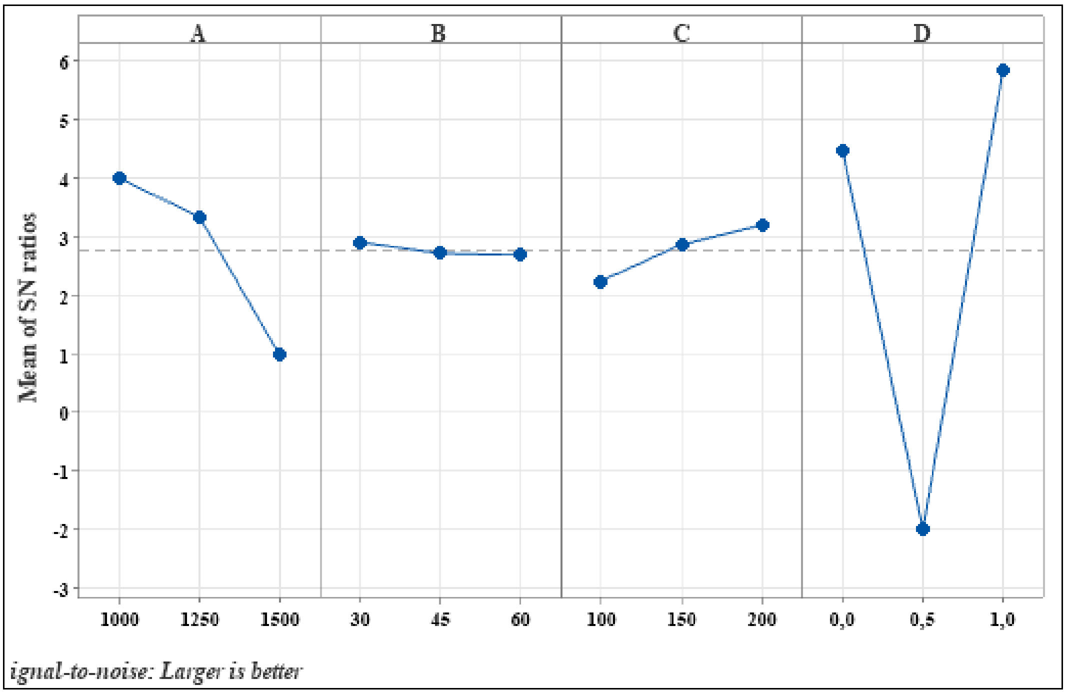

Figure 1. Main effects plot for SN Ratio for Absorbance

Table 7. Response table for SN ratio for SR: (Smaller is better *optimum level)

Level	A	B	C	D
1	**29.04***	**28.57***	31.13	33.41
2	34.31	30.11	**28.58***	30.26
3	29.54	34.21	33.19	**29.22***
Delta	5.27	5.64	4.61	4.19
Rank	2	1	3	4

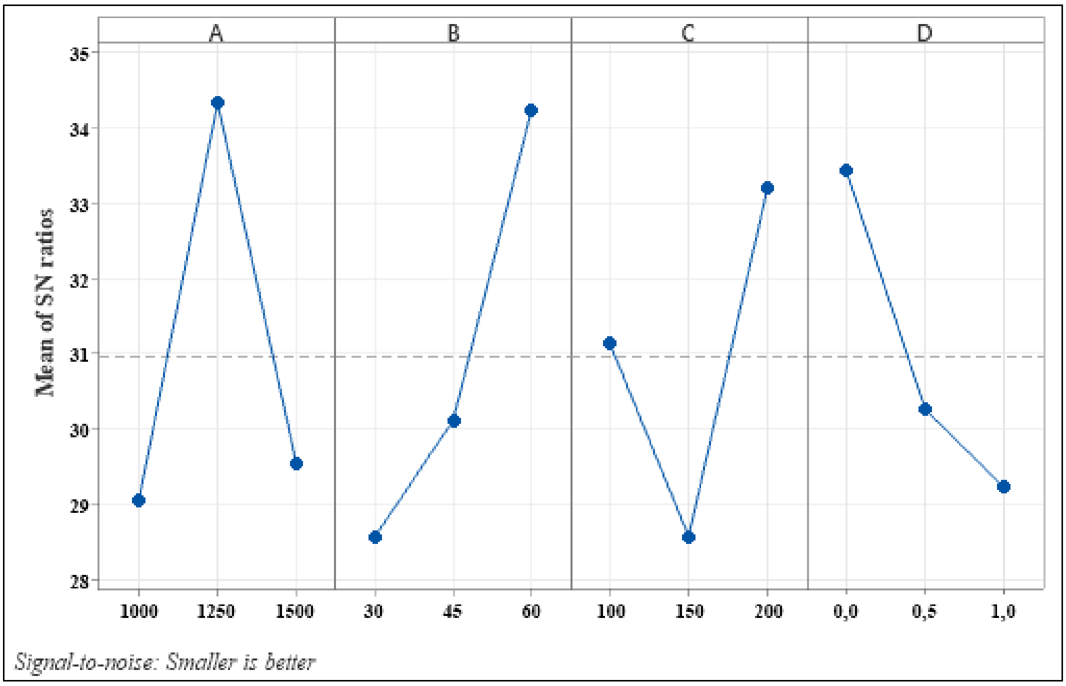

Figure 2. Main effects plot for SN ratio for sedimentation ratio

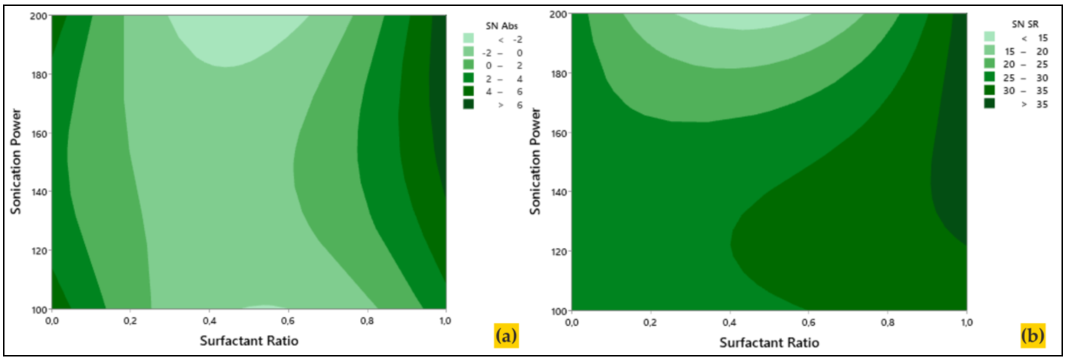

Figure 3. SN Ratio contour plot for: (a) Absorbance; (b) SR

3.2.2. Analysis of Variance (ANOVA)

The ANOVA results for absorbance and sedimentation ratio are shown in **Table 8** and **Table 9**. This analysis uses a 5% significance level and a 95% confidence level. The significance of the controlled factors in ANOVA is determined by comparing the F-value of each control factor. The last column in each table displays the contribution of each independent variable, indicating the degree of influence on the process performance. Based on **Table 8** and **Figure 3**, the most influential factor on high absorbance is sonication power, with a percentage of 31.45%, followed by surfactant concentration (28.43%), sonication time (24.11%), and stirrer speed (16.01%). For the sedimentation ratio, as shown in **Table 9** and **Figure 4**, the most dominant factors are surfactant concentration, sonication power, stirrer speed, and sonication time, with percentage contributions of 82.60%, 13.29%, 3.10%, and 1.01%, respectively.

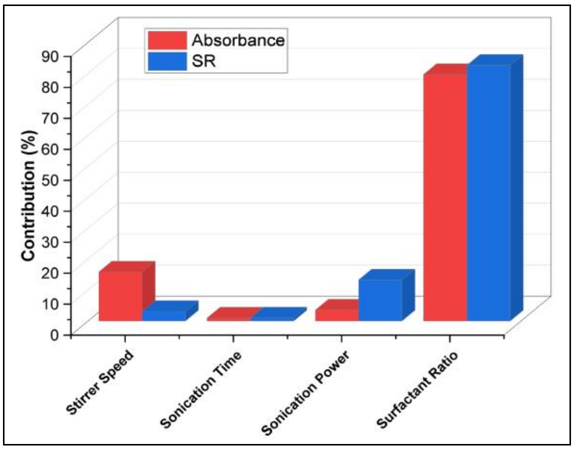

Figure 4. Contribution for Absorbance and SR

Table 8. ANOVA result for Absorbance (*pooled factor)

Source	Deg. of Freedom (DF)	Sum of Squares (SS)	Variance (V)	F-Value	Contribution
A	2	0.46096	0.23048	16.37	15.86%
B	2	0.02816*	-	-	-
C	2	0.10282	0.05141	3.65	3.54%
D	2	2.31429	1.15714	82.20	79.63%
Pooled Error	2	0.02816	0.01408		0.97%
Total	8	2.90622			

Table 9. ANOVA result for sedimentation ratio (*pooled factor)

Source	Deg. of Freedom (DF)	Sum of Squares (SS)	Variance (V)	F-Value	Contribution
A	2	0.000052	0.000026	0.04	3.10%
B	2	0.000017	0.000009	0.01	1.01%
C	2	0.000223	0.000112	0.16	13.29%
D	2	0.001386*	-	-	-
Pooled Error	2	0.001386	0.000693		82.60%
Total	8	0.001678			

3.2.3. Confirmation Test

Confirmation tests were conducted by selecting the optimum parameters derived from the Taguchi method. The optimal parameter combinations by the Taguchi method for Abs and SR are A1B1C3D3 and A1B1C2D3, respectively. These two combinations were experimentally tested as the 10th and 11th experiments. The results of these experiments are shown in **Table 10**. Bothresults demonstrate higher absorbance values and lower SR compared to the L9 design, indicating that the Taguchi optimization for single-objective was successful.

Table 10. Confirmation test result

Combination	Absorbance	SR
A1B1C3D3	2.9	0.012
A1B1C2D3	2.6	0.011

3.3. Multi-objective Optimization

Table 11 shows the results of the grey relational analysis (GRA) on the L9 orthogonal array. The highest grey relational value was obtained in the 6th experiment (0.748). This indicates that the highest absorption value and the lowest sedimentation ratio were achieved in the 6th experiment of the L9 orthogonal array. Additionally, the "larger is better" characteristic of the SN ratio is used to determine the optimal combination in multiple response optimization because higher values are desired. The SN results are displayed in **Table 11**, with the response shown in **Table 12** and **Figure 5**. Because the highest SN criteria represent the best results, the optimal conditions are when the stirrer speed is 1250 rpm, the sonication time is 60 minutes, the sonication power is 100 watts, and the surfactant ratio is 1. The most influential factor was determined through ANOVA evaluation, with results shown in **Table 12**. Surfactant concentration was the most influential factor, contributing up to 54.1%. These results align with the single-objective optimization findings, indicating that surfactant concentration is the most significant factor in nanofuel stability.

Table 11. GRA result

Exp.	Normalized Data		Deviation Sequence		Grey Relation Coefficient		Grey Relation	SN Ratio	Rank
No.	Abs.	SR	Abs.	SR	Abs.	SR	Grade		
1	0.693	0.000	0.307	1.000	0.619	0.333	0.476	-6.441	6
2	0.139	0.433	0.861	0.567	0.367	0.469	0.418	-7.579	9
3	1.000	1.000	0.000	0.000	1.000	1.000	1.000	0.000	1
4	0.880	0.961	0.120	0.039	0.806	0.927	0.866	-1.245	2
5	0.705	0.343	0.295	0.657	0.629	0.432	0.530	-5.508	4
6	0.060	0.491	0.940	0.509	0.347	0.495	0.421	-7.507	8
7	0.000	0.755	1.000	0.245	0.333	0.671	0.502	-5.985	5
8	0.482	0.759	0.518	0.241	0.491	0.675	0.583	-4.686	3
9	0.404	0.266	0.596	0.734	0.456	0.405	0.431	-7.318	7

3.3.1. SN Ratio for GRG

The response table for the SN ratio on the GRG is shown in **Table 12** and plotted in **Figure 3**. The "larger is better" criterion was selected for GRG because a higher GRG value represents higher absorbance and a lower sedimentation ratio, indicating a stable nanofuel. The highest SN ratio for factors A and B was achieved at level 1, with values of -4.673 and -4.557, respectively. For factors

C and D, the highest SN ratio was at level 3, with values of -3.831 and -1.977, respectively. The best combination of the four factors that produces the highest GRG value is A1B1C3D3. The inconsistency between GRA and GRG results reflects differences in their evaluation methods. GRA focuses on individual experimental results, whereas GRG optimizes parameter levels for robustness across multiple runs. Despite this, the differences in responses are minor (Abs: 2.35 vs. 2.9; SR: 0.0124 vs. 0.012), indicating that both methods yield effective outcomes. The GRG result (A1B1C3D3) is chosen for its balanced optimization across objectives.

Table 12. Response table for SN ratio for GRG

Level	A	B	C	D
1	**-4.673**	**-4.557**	-6.211	-6.422
2	-4.754	-5.924	-5.380	-7.023
3	-5.996	-4.942	**-3.831**	**-1.977**
Delta	1.323	1.367	2.380	5.046
Rank	4	3	2	1

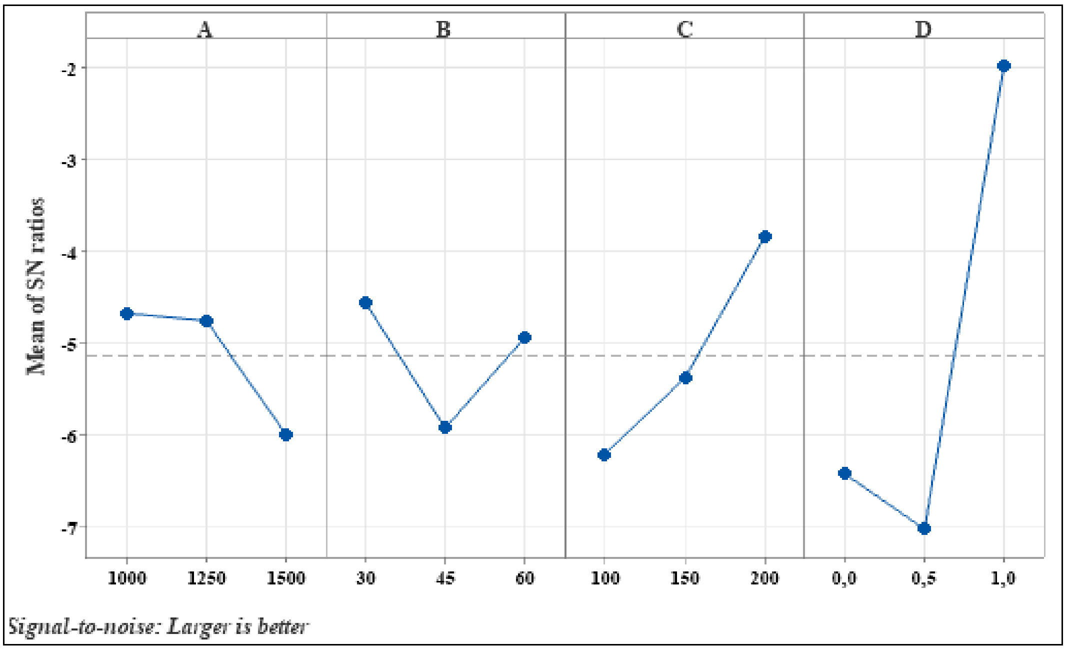

Figure 5. Main effects plot for SN ratio for GRG

3.3.2. Analysis of Variance (ANOVA) for GRG

Table 13 displays the ANOVA results for GRG for each factor. The surfactant ratio (D) is the largest contributor to the high GRG value, with a percentage of 71.5%. The second largest contributing factor is sonication power (C), with 14.54%. Stirrer speed contributes 7.6%, and finally, sonication time contributes 6.35% to the GRG value.

Table 13. ANOVA results for GRG (*pooled factor)

Source	Deg. of Freedom (DF)	Sum of Squares (SS)	Variance (V)	F-Value	Contribution
A	2	0.02672*	-	-	-
B	2	0.02235	0.01117	0.84	6.35%
C	2	0.05111	0.02556	1.91	14.54%
D	2	0.25129	0.12564	9.40	71.5%
Pooled Error	2	0.02672	0.01336		7.6%
Total	8	0.35147			

3.4. Discussion

The Taguchi method provided significant insights into the influence of various parameters on nanofuel stability. For absorbance, the optimal conditions were identified as stirrer speed of 1000 RPM, sonication time of 30 minutes, sonication power of 200 watts, and surfactant ratio of 1. These findings are consistent with those of Shaikh and Patel [30], who demonstrated that higher sonication power significantly improves nanoparticle dispersion, enhancing fuel stability. Similarly, Rao et al. [31] reported that surfactant concentration is a critical factor in improving the stability of biofuel, which aligns with the dominant contribution of surfactant ratio (79.63%) observed in this study. Furthermore, the optimal sonication time of 30 minutes is in agreement with Saleem et al. [32], who found that this duration is sufficient to achieve a stable nanofuel solution without agglomeration. While higher sonication power enhances dispersion, it may also increase energy costs and alter viscosity. Similarly, excessive surfactant use could affect fuel compatibility. Balancing these factors is crucial for practical applications.

The critical roles of sonication power and surfactant concentration in enhancing absorbance can be attributed to their effects on the dispersion and stabilization of MWCNTs in the palm oil matrix. The optimal sonication power of 200W and surfactant ratio of 1 were identified as maximizing nanoparticle dispersion and stability. High sonication power reduces nanoparticle size, while sufficient surfactant concentration minimizes interparticle attractions, as supported by Shaikh and Patel [30]. Higher sonication power facilitates better dispersion of MWCNTs in the base fluid by reducing the size of nanoparticles through fragmentation, which increases the surface area [35]. Surfactant concentration also plays a crucial role in nanofuel by reducing the surface tension between the oil and MWCNTs. Higher surfactant concentrations improve the wettability of MWCNTs, ensuring they remain suspended and preventing sedimentation. This is evident from the ANOVA results, where surfactant concentration contributed 82.6% to the reduction in sedimentation ratio and 28.43% to the increase in absorbance, highlighting its dominance in maintaining nanofuel stability.

GRA facilitates multiple objectives, addressing both absorbance and sedimentation ratios simultaneously. The optimal conditions from GRA are a stirrer speed of 1000 RPM, a sonication time of 30 minutes, a sonication power of 200 watts, and a surfactant ratio of 1. These conditions are consistent with the results of single-objective optimization, particularly emphasizing the dominant influence of surfactants on stability. The fact that both the Taguchi method and GRA yielded similar optimal parameters strongly validates the robustness of the results, as the methods complement and reinforce each other.

These findings are pivotal for advancing nanofuel technology, particularly in enhancing fuel stability. The identified optimal parameters provide a robust framework for producing high stability nanofuels, potentially contributing to more efficient and sustainable energy solutions. The optimized parameters could improve combustion efficiency by ensuring uniform fuel-air mixtures. Reduced sedimentation may also enhance thermal conductivity and minimize emissions. Future studies should validate these implications in real-world conditions.

4. Conclusion

This research optimized the preparation parameters of palm oil and MWCNT-based nanofuel using a Taguchi-GRA combination. The single-objective optimization results showed that the best parameter combination for the highest absorption was A1B1C3D3, while A1B1C2D3 yielded the lowest sedimentation ratio. ANOVA analysis revealed that surfactant concentration played the most significant role in nanofuel stability, contributing 79.63% to absorbance and 82.60% to sedimentation ratio. Multi-objective optimization using GRA confirmed the dominance of surfactant concentration, contributing 71.5% to the Grey Relational Grade. When compared with existing studies, the results of this research align with the critical role of sonication power, surfactant concentration, and optimal sonication time. These similarities highlight the robustness and reliability of the optimization methodology used in this study. Additionally, the differences observed emphasize the unique contribution of this research in integrating Taguchi and GRA methods for nanofuel stability optimization. While the Taguchi and GRA methods generally provided consistent optimization results, minor discrepancies were observed in specific cases, such as between GRA rankings and SN ratio results. These differences were addressed by prioritizing GRG results, which offer a balanced approach to multi-objective optimization. Further validation across diverse scenarios is recommended to confirm the reliability of these methods. This research provides a strong foundation for the development of stable nanofuels, potentially enhancing energy efficiency and sustainability. The findings offer valuable practical guidelines for real-world applications and pave the way for future studies to explore scalability and performance in larger systems.

Authors' Declaration

Authors' contributions and responsibilities - The authors made substantial contributions to the conception and design of the study. The authors took responsibility for data analysis, interpretation, and discussion of results. The authors read and approved the final manuscript.

Funding – This research was funded by DRTPM Kementerian Pendidikan, Kebudayaan, Riset, dan Teknologi 2023.

Availability of data and materials - All data is available from the authors.

Competing interests - The authors declare no competing interest.

Additional information – No additional information from the authors.

References

[1] A. A. Permanasari, A. F. Wahidin, H. Ismail, E. Komara, P. Puspitasari, and G. A. Lorenzo, "Comparative Analysis of the Effect Dual Spark Ignition and Single Spark Ignition on Performance and Exhaust Emissions in Bioethanol-Fueled Engines," *Journal of Mechanical Engineering Science and Technology (JMEST)*, vol. 8, no. 1, pp. 123–137, 2024, doi: 10.17977/um016v8i12024p123.

[2] A. F. Alphanoda, E. A. Pane, and A. Riyanto, "The Role of Banana Peel Surface Pores through Increasing Temperature for Efficient Hydrogen Production," *Journal of Mechanical Engineering Science and Technology (JMEST)*, vol. 8, no. 2, p. 421, Nov. 2024, doi: 10.17977/um016v8i22024p421.

[3] S. Marianingsih, F. Mar'i, and H. Y. Nanlohy, "Artificial Neural Network-Based Modeling of Performance Spark Ignition Engine Fuelled with Bioethanol and Gasoline," *Journal of Mechanical Engineering Science and Technology (JMEST)*, vol. 7, no. 2, p. 190, 2023, doi: 10.17977/um016v7i22023p190.

[4] M. A. Raehan, H. Riupassa, and H. Y. Nanlohy, "Captivating Combustion Traits of Bio-Oil Droplets Enriched with Bio-Additives from the Areca Shell Waste," *Journal of Mechanical Engineering Science and Technology (JMEST)*, vol. 8, no. 2, p. 384, Nov. 2024, doi: 10.17977/um016v8i22024p384.

[5] J. L. Ramos, B. Pakuts, P. Godoy, A. García-Franco, and E. Duque, "Addressing the energy crisis: using microbes to make biofuels," *Microbial Biotechnology*, vol. 15, no. 4, pp. 1026–1030, Apr. 2022, doi: 10.1111/1751-7915.14050.

[6] M. M. Y. Romaz, S. Sukarni, and R. Wulandari, "Characteristics of Liquid Products from Spirulina platensis Pyrolysis under Microwave Irradiation with Activated Carbon Additive," *Journal of Mechanical Engineering Science and Technology (JMEST)*, vol. 8, no. 2, p. 503, Nov. 2024, doi: 10.17977/um016v8i22024p503.

[7] S. Suardi, R. J. Ikhwani, and A. P. R. Aulia, "Effect of Temperature Variations of Corn (Maize) Oil Biodiesel on Torque Values and Thermal Efficiency of Diesel Engines," *Journal of Mechanical Engineering Science and Technology (JMEST)*, vol. 7, no. 1, p. 87, Jun. 2023, doi: 10.17977/um016v7i12023p087.

[8] A. J. Alyaseri, "The Reality And Future of Renewable Energy Sources in The Global Energy Market," *Akkad Journal Of Multidisciplinary Studies*, vol. 1, no. 4, pp. 270–283, Jun. 2022, doi: 10.55202/ajms.v1i4.98.

[9] S. Thanikodi, S. Rathinasamy, J. Giri, A. K. Jagadeesan, and E. Makki, "Biodiesel Production from Food Industrial Waste of Soybean Oil using a Lipase-nanoparticle Bio-composite Catalyst," *Automotive Experiences*, vol. 7, no. 2, pp. 189–206, 2024, doi: 10.31603/ae.10707.

[10] S. Suherman *et al.*, "A Review of Properties, Engine Performance, Emission Characteristics and Material Compatibility Biodiesel From Waste Cooking Oil (WCO)," *Automotive Experiences*, 2023, doi: 10.31603/ae.10128.

[11] S. Supriyadi, P. Purwanto, D. D. Anggoro, and H. Hermawan, "The Effects of Sodium Hydroxide (NaOH) Concentration and Reaction Temperature on The Properties of Biodiesel from Philippine Tung (Reutealis Trisperma) Seeds," *Automotive Experiences*, vol. 5, no. 1, pp. 57–67, 2022, doi: 10.31603/ae.5986.

[12] J. Milano *et al.*, "A Comprehensive exploration of jatropha curcas biodiesel production as a viable alternative feedstock in the fuel industry – Performance evaluation and feasibility analysis," *Mechanical Engineering for Society and Industry*, vol. 4, no. 1, pp. 17–37, Apr. 2024, doi: 10.31603/mesi.10610.

[13] F. A. Malla, S. A. Bandh, S. A. Wani, A. T. Hoang, and N. A. Sofi, "Biofuels: Potential Alternatives to Fossil Fuels," in *Biofuels in Circular Economy*, Singapore: Springer Nature Singapore, 2022, pp. 1–15.

[14] A. Kolakoti, M. Setiyo, and B. Waluyo, "Biodiesel Production from Waste Cooking Oil: Characterization, Modeling and Optimization," *Mechanical Engineering for Society and Industry*, vol. 1, no. 1, pp. 22–30, 2021, doi: 10.31603/mesi.5320.

[15] E. Kwao-Boateng, M. Agbedam, A. N. P. Agyemang, E. Acquah, K. A. Ofori, and A. T. Tagoe, "Comparative analysis of palm kernel and waste cooking oils for biodiesel production as an alternative fuel to conventional diesel fuel," *Journal of the Ghana Institution of Engineering (JGhIE)*, vol. 23, no. 2, pp. 1–5, Jun. 2023, doi: 10.56049/jghie.v23i2.8.

[16] A. C. Ajie, M. M. Ojapah, and E. O. Diemuodeke, "Effect of Palm Oil Biodiesel Blends on Engine Emission and Performance Characteristics in an Internal Combustion Engine," *Open Journal of Energy Efficiency*, vol. 01, no. 01, pp. 13–24, 2023, doi: 10.4236/ojee.2023.11002.

[17] A. Chukwudi Okwuchukwu, "Engine Performance Analysis of Palm Kernel Oil-Based Biodiesel Blends on Speed Variations of a 4-Cylinder Engine at Constant Torque," *Journal of Advance Research in Mechanical & Civil Engineering*, vol. 9, no. 4, pp. 6–11, Apr. 2023, doi: 10.53555/nnmce.v9i4.1640.

[18] S. Suardi, M. Purwanto, A. Y. Kyaw, W. Setiawan, M. U. Pawara, and A. Alfawan, "Biodiesel Production from POME (Palm Oil Mill Effluent) and Effects on Diesel Engine Perfor-mance," *International Journal of Marine Engineering Innovation and Research*, vol. 7, no. 4, Dec. 2022, doi: 10.12962/j25481479.v7i4.14492.

[19] S. Pambudi, N. Ilminnafik, S. Junus, and M. N. Kustanto, "Experimental Study on the Effect of Nano Additives γAl2O3 and Equivalence Ratio to Bunsen Flame Characteristic of Biodiesel from Nyamplung (Calophyllum Inophyllum)," *Automotive Experiences*, vol. 4, no. 2, pp. 51–61, 2021, doi: 10.31603/ae.4569.

[20] A. T. Mohammed, M. F. M. Said, N. Othman, A. C. Opia, and I. Veza, "Feasibility Study of Biofuel Incorporated Nanoparticles as Sustainable IC Engine Fuel: Opportunities and Challenges - An overview," *Automotive Experiences*, vol. 6, no. 1, pp. 94–121, Apr. 2023, doi: 10.31603/ae.7846.

[21] S. Daud, M. A. Hamidi, and R. Mamat, "Design of Experiment to Predict the Effects of Graphene Nanoplatelets Addition to Diesel Engine Performance," *Automotive Experiences*, vol. 5, no. 3, pp. 467–476, Sep. 2022, doi: 10.31603/ae.6263.

[22] C. Antony, D. Ghana, and A. Kumar, "Synthesis of nanoparticles in dual biodiesel and enchancement in performances and emission characteristics," *Zastita materijala*, vol. 64, no. 1, pp. 22–29, 2023, doi: 10.5937/zasmat2301022J.

[23] J. Senthilkumar, K. Dharun, T. Sanchit Kumar, R. Suresh Kumar, N. Jayanthi, and S. Venkatesh, "Impact of nano catalyst in the biodiesel production for direct injection diesel engine: A review," *Environmental Quality Management*, vol. 33, no. 4, pp. 257–266, Jun. 2024, doi: 10.1002/tqem.22057.

[24] A. Lakhera *et al.*, "Optimization of diesel engine performance and emission characteristics with cerium oxide nanoparticles mixed waste cooking oil biodiesel blends," *International Journal of Engine Research*, vol. 24, no. 11, pp. 4521–4531, Nov. 2023, doi: 10.1177/14680874221133223.

[25] M. G. Bidir, M. Narayanan Kalamegam, M. S. Adaramola, F. Y. Hagos, and R. C. Singh, "Comparative study on the effect of nanoparticles in ternary fuel blends on combustion, performance, and emissions characteristics of diesel engine," *International Journal of Engine Research*, vol. 24, no. 11, pp. 4509–4520, Nov. 2023, doi: 10.1177/14680874221132963.

[26] E. Espinel Blanco, R. C. Vázquez-Fletes, J. S. Rudas, M. I. Ardila Marín, L. M. Hoyos-Palacio, and J. A. Carlos Cornelio, "Effect of the concentration of carbon nanotubes (CNTs) on the rheological behavior in a lubricating oil of plant-derived lubricant," *Journal of Dispersion Science and Technology*, vol. 45, no. 7, pp. 1444–1454, May 2024, doi: 10.1080/01932691.2023.2215307.

[27] D. Nurmukan, M.-V. Tran, Y. M. Hung, G. Scribano, and C. T. Chong, "Effect of multi-walled carbon nanotubes on pre-vaporized palm oil biodiesel/air premixed flames," *Fuel Communications*, vol. 8, p. 100020, Sep. 2021, doi: 10.1016/j.jfueco.2021.100020.

[28] M. Amsal, M.-V. Tran, Y.-M. Hung, and G. Scribano, "Experimental study of evaporation of palm biodiesel with multi-walled carbon nanotubes additives at elevated temperatures," *International Journal of Environmental Science and Technology*, vol. 19, no. 7, pp. 6611–6624, Jul. 2022, doi: 10.1007/s13762-021-03465-1.

[29] C. Rao. Seela, "Carbon Nanotubes (MWCNTs) Added Biodiesel Blends: An Engine Analysis," *RASAYAN Journal of Chemistry*, vol. 15, no. 02, pp. 1009–1020, 2022, doi: 10.31788/RJC.2022.1526882.

[30] M. A. Shaikh and V. R. Patel, "Experimental studies on ethanol solubility and nanoparticle (NP)

stability in diesel fuel," *Chemical Engineering Research and Design*, vol. 188, pp. 105–129, Dec. 2022, doi: 10.1016/j.cherd.2022.09.030.

[31] M. S. Rao, C. S. Rao, and A. S. Kumari, "Synthesis, stability, and emission analysis of magnetite nanoparticle-based biofuels," *Journal of Engineering and Applied Science*, vol. 69, no. 1, p. 79, Dec. 2022, doi: 10.1186/s44147-022-00127-y.

[32] A. B. Saleem, R. Mamat, F. Y. Hagos, A. A. Abdullah, and A. Arman, "Investigation of the stability of cerium oxide in diesel fuel for nano-enhanced fuel formulation," in *II International Scientific Forum On Computer And Energy Sciences (WFCES-II 2021)*, 2022, p. 030014, doi: 10.1063/5.0099886.

[33] L. Bao *et al.*, "Experiments on macroscopic spray characteristics of diesel-ethanol with dispersed cerium nanoparticles," *Journal of the Energy Institute*, vol. 93, no. 6, pp. 2186–2196, Dec. 2020, doi: 10.1016/j.joei.2020.06.001.

[34] G. Singh, E. Lopes, N. Hentges, D. Becker, and A. Ratner, "Experimental Investigation of the Settling Characteristics of Carbon and Metal Oxide Nanofuels," *Journal of Nanofluids*, vol. 8, no. 8, pp. 1654–1660, Dec. 2019, doi: 10.1166/jon.2019.1715.

[35] S. U. Ilyas, R. Pendyala, and N. Marneni, "Stability of Nanofluids," in *Engineering Applications of Nanotechnology*, 2017, pp. 1–31.

[36] R. Sadeghi, S. G. Etemad, E. Keshavarzi, and M. Haghshenasfard, "Investigation of alumina nanofluid stability by UV–vis spectrum," *Microfluidics and Nanofluidics*, vol. 18, no. 5–6, pp. 1023–1030, May 2015, doi: 10.1007/s10404-014-1491-y.

[37] P. C. Mukesh Kumar, K. Palanisamy, and V. Vijayan, "Stability analysis of heat transfer hybrid/water nanofluids," *Materials Today: Proceedings*, vol. 21, pp. 708–712, 2020, doi: 10.1016/j.matpr.2019.06.743.

[38] A. R. I. Ali and B. Salam, "A review on nanofluid: preparation, stability, thermophysical properties, heat transfer characteristics and application," *SN Applied Sciences*, vol. 2, no. 10, p. 1636, 2020, doi: https://doi.org/10.1007/s42452-020-03427-1.

[39] W. Purwanto, T. Sugiarto, H. Maksum, M. Martias, M. Nasir, and A. Baharudin, "Optimal Design of Rotor Slot Geometry to Reduce Rotor Leakage Reactance and Increase Starting Performance for High-Speed Spindle Motors," *Advances in Electrical and Electronic Engineering*, vol. 17, no. 2, pp. 96–105, Jun. 2019, doi: 10.15598/AEEE.V17I2.3170.

[40] M. T. Ulhakim, G. Triyanto, F. Arrozak, R. Huseri, S. Sukarman, and R. Ridwan, "High efficiency process on the salted eggs preparation through the parameters optimization by using taguchi method," *BIS Energy and Engineering*, vol. 1, pp. V124017–V124017, 2024, doi: 10.31603/biseeng.46.

[41] W. Warju, S. R. Ariyanto, M. Y. Pratama, and K. R. Haratama, "Optimization of Metallic Catalytic Converters to Reduce CO Emissions and Increase Engine Power," *Automotive Experiences*, vol. 7, no. 2, pp. 299–309, Sep. 2024, doi: 10.31603/ae.11587.

[42] Sukarman *et al.*, "Optimization of tensile-shear strength in the dissimilar joint of Zn-coated steel and low carbon steel," *Automotive Experiences*, vol. 3, no. 3, pp. 115–125, 2020, doi: 10.31603/ae.v3i3.4053.

[43] S. R. Ariyanto, S. Suprayitno, and R. Wulandari, "Design of Metallic Catalytic Converter using Pareto Optimization to Improve Engine Performance and Exhaust Emissions," *Automotive Experiences*, vol. 6, no. 1, pp. 200–2015, Apr. 2023, doi: 10.31603/ae.7977.

[44] A. D. Shieddieque, Sukarman, Mardiyati, B. Widyanto, and Y. Aminanda, "Multi-objective Optimization of Sansevieria Trifasciata FibreReinforced Vinyl Ester (STF/VE) Bio-composites for the Sustainable Automotive Industry," *Automotive Experiences*, vol. 5, no. 3, pp. 288–303, 2022, doi: 10.31603/ae.7002.

[45] T. Dagdevir and V. Ozceyhan, "Optimization of process parameters in terms of stabilization and thermal conductivity on water based TiO2 nanofluid preparation by using Taguchi method and Grey relation analysis," *International Communications in Heat and Mass Transfer*, vol. 120, p. 105047, Jan. 2021, doi: 10.1016/j.icheatmasstransfer.2020.105047.

[46] K. Soorya Prakash, P. M. Gopal, and S. Karthik, "Multi-objective optimization using Taguchi based grey relational analysis in turning of Rock dust reinforced Aluminum MMC," *Measurement*, vol. 157, p. 107664, Jun. 2020, doi: 10.1016/j.measurement.2020.107664.